Proceedings of the 2015
IEEE Conference on Robotics and Biomimetics
Zhuhai, China, December 6-9, 2015

A Method to Implement Biomimetic Control for a SMA Springs Array *

Shenshun. Ying, Shiming Ji, Donghai Cai, Guanjun. Bao and Zhun Fan, *Member, IEEE*

***Abstract*—Artificial muscle works in a much different way from motor drive, and shows a good prospect of the application in intelligent devices and biomimetic robot fields. It is usually clustered and hard to control. This paper focus on the biomimetic control method of a Shape Memory Alloy (SMA) springs array that has characteristics of artificial muscle. Material characteristics of SMA are firstly analyzed, and attached platform with a 5×3 SMA springs array prototype is then set up. Secondly, after analyzing the motor control behavior of skeletal muscle, this paper establishes a biomimetic method to control the signal and energy, and presents the design result of control system including a programmable logic controller (PLC) based control device, a configuration software based graphical user interface (GUI) and control programming. Experiment is finally designed to explore the responsiveness and stability of the control system, and output displacement and force of the SMA springs array are measured. The test result proves the feasibility and real time of this control method and device presented in this paper.**

I. Introduction

SMA has high energy density, small size, the possibility of applying the force directly without the use of transmission, and a unique two-phase (martensite/austenite) property. Taking advantage of these excellent characteristics, SMA has been used for robotic hands [1], robotic starfish [2], robotic sea lamprey [3], crawling microbots [4], soft robot[5], etc. However, recovery force produced by single SMA actuator is too little to meet applications that require large output power or multiple degrees of freedom. By contrast, a group of SMA actuators, namely SMA actuators array, has large strain and big tension property, and the force/displacement output can be tailored by activating the actuator cells in a coordinated manner [6, 7]. The study on array actuators mainly includes (1) Topology design methodology, namely how many small cells interconnected in various layouts, to achieve muscle-like motion, and (2) control method, namely how to exhaust force/ displacement output as required for an array actuators with given topology. Many researchers have studied on these issues. For example, Mosley formed one powerful muscle mechanically by bundling a series of SMA wires in parallel [8]. Cho et al studied systematically cellular actuators including a cellular design for a robotic hand with 11 SMA actuators [1] and a broadcast-probability approach to the control of vast DOF cellular actuators [9]. So far, the structure design of an actuators array is relatively mature, topologies such as series, parallel, hybrid structure, as well as the diamond amplification mechanism, have been widely examined. However, when the number of actuator cells to be controlled increase, even in the case of an ideal linear actuator, the difficulty of control will greatly increases. Some examples testify to this effort [3, 10].

[11] presents biologically-inspired cell array actuators. In this work all cells were identical and the topology of the cell array actuator, represented compactly using a two row set of matrices or ‘‘fingerprint’’, differentiated static properties such as displacement, force capacity, force discretization, and robustness. The cells were operated using a bi-stable stochastic all-on all-off broadcast control method to reduce wiring complexity, control signals, and hysteresis error. [12] presents expanded fingerprint method allowing the dynamics to be calculated with less human effort, less computational effort, and with greater speed, especially when comparing different topologies and cell dynamics. Two different physical SMA based cell array actuators were designed to validate the presented theory. The presented theory provides an intuitive base for future controls work. but was not reliable enough for wider scale implementation.

To gain both large strain and big tension property, we built a SMA springs array [6]. Output properties of the SMA springs array that has a given topology has analyzed, and the experiment data indicated there exists a serious coupling phenomenon within the SMA springs array. In this paper, we focus on the method and device to implement control for the SMA springs array. Our approach is inspired by motor control of skeletal muscle, where nerve impulses and ATP conversion function together. Basing on a SMA springs array with three rows and five columns, the control of signal and energy flow is separately considered, the PLC is used as their automatic control parts, which is ripe and reliable in technology.

II. SMA Springs Array Actuator

SMAs are metals which exhibit two very unique properties: pseudo-elasticity and shape memory effects (SME). These two effects are possible through a solid phase state change from the martensite phase to the austenite one and vice versa. Martensite is the relatively soft and easily deformed phase, which exists at lower temperatures. A deformation of the alloys during this phase will be retained until they are heated. Heating will cause

*.
Manuscript received November 2, 2015. This work is partially supported by the Natural Science Foundation of Zhejiang Province under Grant Y1110953 and LY14E050009.

Shenshun. Ying is with Zhejiang University of Technology,Hangzhou, China. (86-0571-88320831; fax: 86-0571-88320372; e-mail: yss@ zjut.edu.cn).

Shiming. Ji is with Zhejiang University of Technology, Hangzhou, China. (e-mail:jishiming@zjut.edu.cn).

Donghai Cai is with Zhejiang University of Technology,Hangzhou, China. (e-mail:dhcai@zjut.edu.cn).

Guanjun. Bao is with Zhejiang University of Technology, Hangzhou, China. (e-mail:gjbao@zjut.edu.cn).

Zhun. Fan is with Shantou University, Shantou, China. (e-mail:fanzhun@gmail.com).

978-1-4673-9675-2/15/$31.00 © 2015 IEEE

transition to the austenite phase with the consecutive recovery of the original shape. When cooled again, the material returns to the martensite phase without any change in shape until a load is applied on it [3].

During the transition from the martensite to the austenite phase, if the material is prevented from recovering its original shape, it is possible to obtain a force called recovery force which can be relatively high. So during the shape recovery phase it is possible to produce mechanical work. The recovery force and the shape variation have the same direction. There are three kinds of SMA actuators, usually including wire, film and spring. Among them, the SMA springs have relatively large strain and little tensile force.

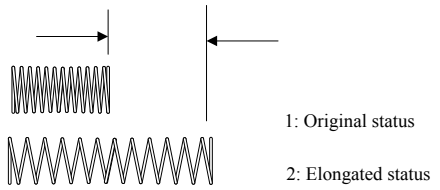

Figure 1. Schematic diagram of a SMA spring

A SMA spring takes either initial or elongated status. It will contract back to initial length under no-load state when suitable current through circuit for several seconds, while it is extended manually to two times of initial length in advance. Figure 1 shows the schematic diagram of a SMA spring.

Figure 2 is the topology diagram of a SMA springs array prototype. The SMA springs array actuator has five rows and three columns, and uses the same specifications of Ni-Ti SMA springs. The cellular building blocks that can be actuated individually and that are connected in series and parallel to move specific points. The total displacement is determined by the integral of strains distributed over the individual building blocks in series. The output force is the summation of the force generation at the individual strands arranged in parallel.

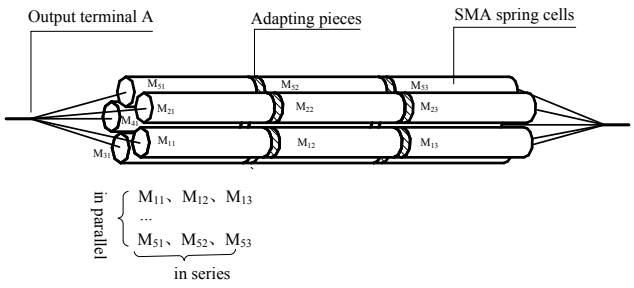

Figure 2. Topology diagram of a 5×3 SMA springs array

III. CONTROL METHOD

A. *Motor Control of Skeletal Muscle*

Figure 3 shows the motor neuron model. When muscles receive the stimulation of nerve impulses, sarcoplasmic reticulum releases calcium, calcium combines with muscle protein, and configuration and location of muscle protein change, the original myosin position changes with it, which makes transverse process of the actin and myosin contact. At the instant of the contact, the atpase is activated, it decomposes ATP and converts chemical energy into mechanical energy, then causes the movement of muscle plasma globulin molecular head, pulls the actin filament, makes the overlap of muscle plasma globulin and actin increase, and the muscle fibers are then shortened, the tendons transmit the contraction force to move a bone. Only when the calcium in sarcoplasm is recovered by sarcoplasmic reticulum, meanwhile there is other ATP molecular combined with plasma globulin molecular head in muscles, muscle plasma globulin head will break away from the actin filament, and muscle then recovers.

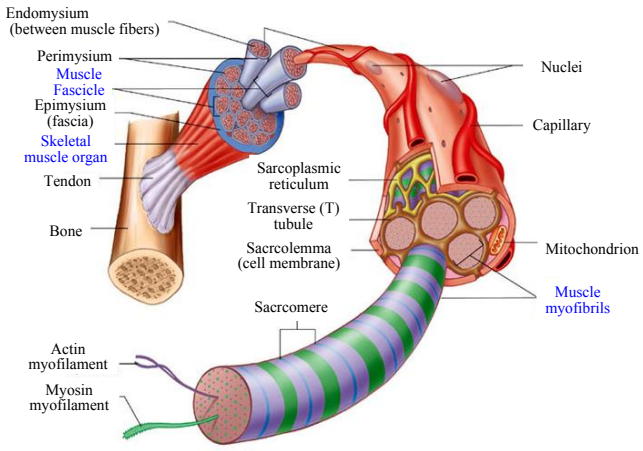

Figure 3. Figure 3. Motor neuron model[13]

By biological neural control of the skeletal muscle, can be summarized that the initiation of a signal depends on nerve and energy depends on ATP.

B. *Biomimetic Control Principle and Method of SMA Springs Array*

Signal flow

Basic **hypothesis** is that user manually inputs signal to select the SMA springs needed to move, then another signal is sent to start actuating. In this way it is easy to obtain various displacements and tension of the SMA springs array when different actuator cells are activated. From this, a signal input device is needed in the control system with a friendly user interface. It must be easy to use, as well as meeting the needs of combining any activated SMA springs topology perfectly. Therefore a simple GUI interface to run on personal computer (PC) is designed, which sends out the control signal.

An external digital controller is needed because the control signal cannot act on SMA spring actuator directly. The digital controller should have number and computing skills, logical processing ability with perfect function and good quality. Three reference schemes are made to meet this need: integrated circuit, PLC and printed circuit board (PCB). By comparison, PLC is selected because it is relatively easy to perform logical processing just through programming, while integrated circuit and PCB have to design additional circuit. CP1H serious PLC and CX-Programmer 9.3 software are the last result of what is selected.

In addition, configuration software is used to design GUI on PC, and the version of the software is Kingview 6.53. Figure 4 shows the control signal flow graph of the SMA springs array.

Energy flow

For SMA springs array, the energy flow is the quantity of heat, which makes SMA spring contract from elongated status. The energy flow management means choosing a suitable heating mode for SMA spring. There are two common heating modes--- one is external heater, the other is ohmic heating. By comparison, we found ohmic heating had simple realization, good effect and high practicality. SMA spring can be activated as long as it connected wires at both ends, and appropriate 5v voltage supply in series with 1 Ω resistor in our SMA spring is suitable, which is validated by preliminary experiments.

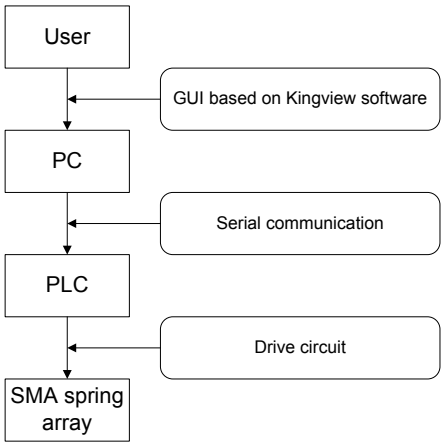

Figure 4. Flow graph of control signal of SMA springs array

Figure 5 presents the structure of ohmic heating device. Among them, 5 v switching power supply, relay, terminal block, and wire compose the power supply circuit loop of SMA spring. The 24 V and 5 V DC switching power supplies respectively provide energy for PLC and SMA springs array. The resistor is used as shut in each DC circuit loop. PLC gets signal from PC to control either connection or disconnection of the each relay, so each SMA spring's actuation can be respectively controlled.

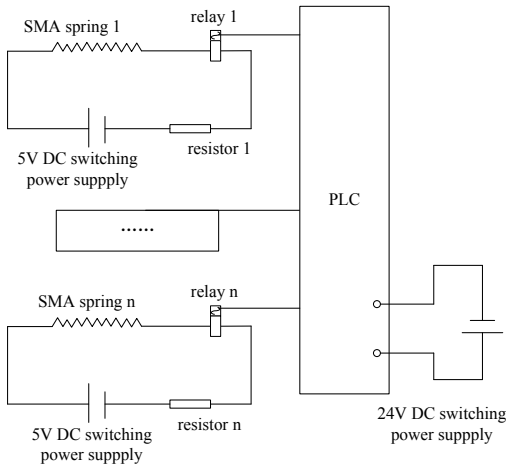

Figure 5. Structure of ohmic heating device

IV. DESIGN AND IMPLEMENTATION OF CONTROL DEVICE

A. Control Device Design Based PLC

The control device mainly include PLC, 24 v relay, relay base, 24 v and 5 v switching power supplies, air switch, terminal blocks, block, guide rail, plate, wire. Figure 5 shows the circuit schematic of control system. CP1H is a product category of Omron PLC, it has 24 inputs and 16 outputs built in, and can be expanded to maximum total of 320 I/O point by using CPM1A Expansion I/O units. In consequence, the control device can easily expand the number of relays according to the scale of SMA springs array, which ensures the advantages of modularity and reconfiguration.

As the communications with higher level device, we connects the CP1H to 232 series port of PC using CIF11 communication module, and the communication protocols are provided by Kingview software.

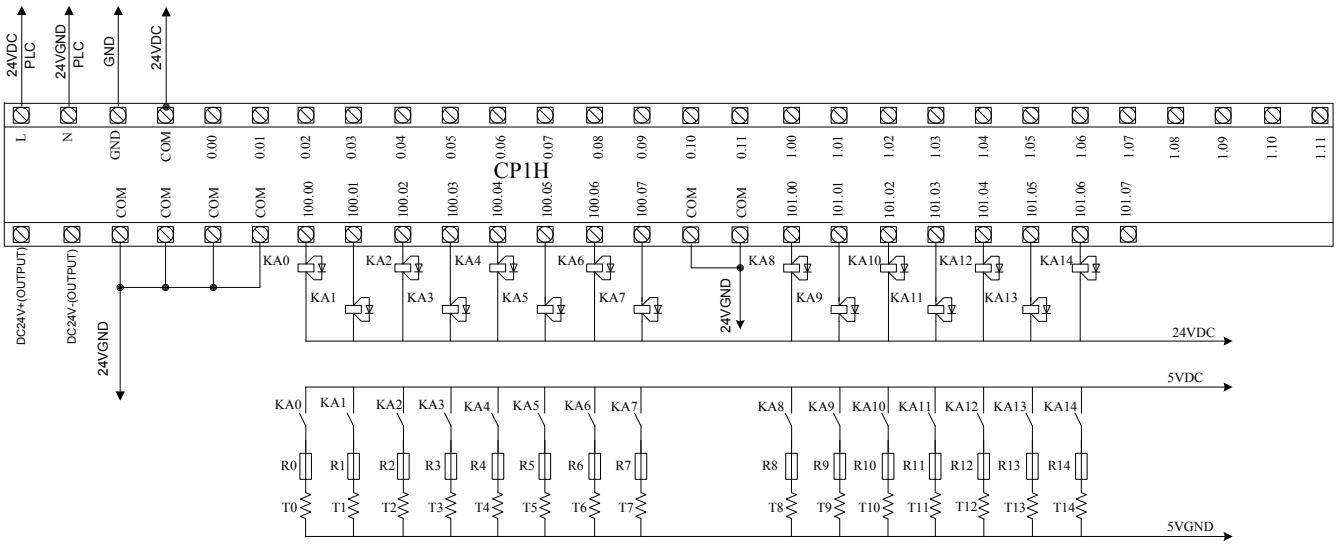

Figure 6. Circuit schematic (T0-T14: SMA spring; R0-R14: resistor; KA0-KA14: relay)

B. GUI Design

GUI is designed based on Kingview software, as shown in Figure 7. The function icons shown in the GUI include three types: selection, command and status display. Corresponding to the fifteen SMA springs of the array, there are fifteen big squares on the right of GUI, and each of them has an associated number. The big blue squares are the SMA springs to be activated, and they will turn black when be clicked, it shows they are selected and will be activated when the control system is power on. Each big blue square has a little red square at left bottom, and it shows that the associated SMA spring has not started electrical heating. When the associated SMA spring starts electrical heating, the little red square turns green.

Due to our SMA springs array has five rows and three columns, as shown in Figure 2, one status indicator below the GUI shows amount of SMA springs to be activated in each row, and the other status indicator lower-left corner identifies the sum of total SMA springs to be activated. Reverse selection and Reset buttons are for selecting or deselecting the SMA springs to be activated. Fan starts up by clicking the Fan button. When the Confirm button is clicked, PC sends out control signal, program of PLC runs, relays conduct external circuit of SMA springs that selected before, and ohmic heating runs. When the Off button is clicked, circuit of SMA spring is open and electricity doesn't go through.

Because too much electricity or heart energy will ruin the shape memory effect of SMA spring, PLC programming must carefully set the loop on-time of SMA spring using timer, and the fan circuit must be switched on as soon as circuit of SMA springs is disconnected.

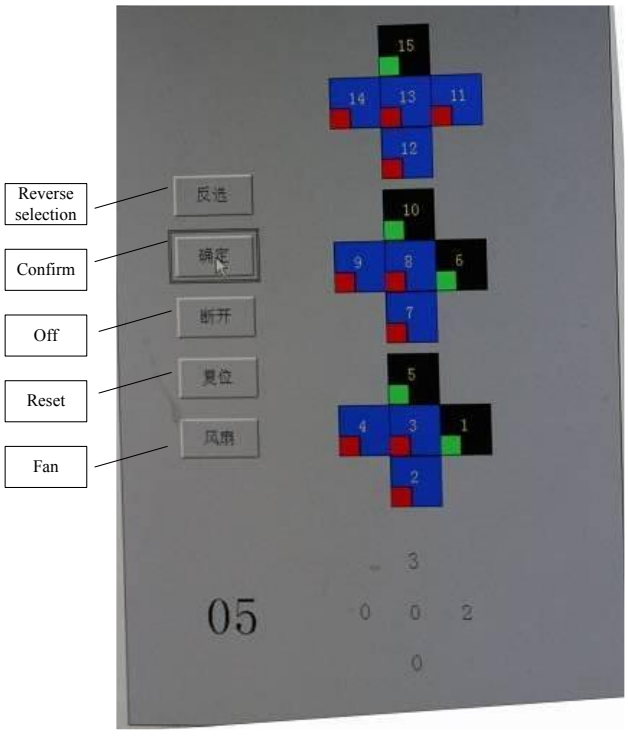

Figure 7. Graphical user interface design of control system

C. PLC programming

The control process of SMA springs array is as follows: firstly, user manually selects the SMA springs to be activated; then, confirm the switch on and start electrical heating; some time later, automatically switch off the selected circuit loop, and open the fan; a little while, turn off the fan. These features must be realized in PLC programming.

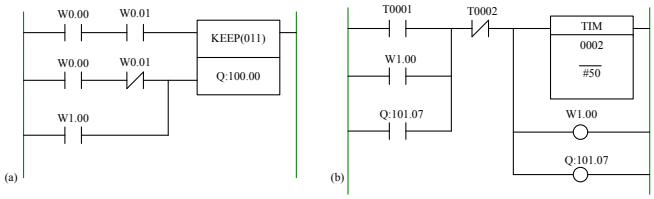

Figure 8. Sample program of PLC programming (a) Selection and confirming command; (b) Fan on-off control

Figure 8 shows two sample programs of software design. They correspond to selection and confirming command, fan on/off control, respectively. Figure 8 (a) is the control program of SMA spring one (see Figure 6). When big square one is selected and displayed in black, the assignment of w0.01 should be kept at 1. Just switch on Confirm button in GUI based on Kingview software, w0.00 has been assigned the value 1, then I/O port 100.00 of PLC will be kept at 1, and the related relay of external circuit close, the SMA spring circuit is closed for ohmic heating. If the big square has not been selected, the I/O port 100.00 will be kept at 0, even if the Confirm button is clicked. At this time, external circuit is open, and there is no ohmic heating in the SMA spring.

V. EXPERIMENT

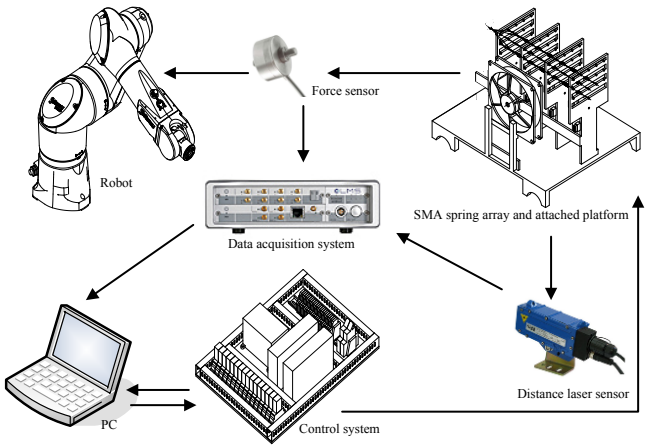

Figure 9. Experiment setup

An experiment is designed to explore the responsiveness and stability of the control system. Figure 9 shows the experiment setup, which includes the following parts: SMA springs array and attached platform, control system, PC, robot, LMS SCADAIII-305 frontend system, distance laser sensor and force sensor. Among them, distance laser sensor, force sensor, robot and LMS SCADAS III frontend compose the measurement system. When different actuator cells are activated, output displacement and force of the SMA springs array are measured. Force sensor is mounted at the end of the robot while connects to the output line of the SMA springs

array. The robot applies the drag force produced by SMA springs array on the force sensor, and produces uniform linear motion for force sensor to offset the inertia force. Table 1 presents the specifications of the test system.

TABLE I. SPECIFICATIONS OF TEST SYSTEM

Setup	Specification	Performance
PC	Dell /M90	
Robot	MotoMAN-H20	Load: 20 Kg Maximum attainable radius: 1717 mm
The frontend	SCADAS III-305	24 channels Max sampling frequency: 204.8 kHz Maximum bandwidth: 92 kHz
Analysis system	LMS.Test.Lab 7.0	
Force sensor	PCB 208C01	Sensitivity: 112mV/N Measurement Range: 45 N Resolution ratio: 0.00045 N-rms
Distance laser sensor	LK-GD500	Measurement Range: ±20mm Storage cycle (p) Sampling: 20 ms

Figure 10 shows the structure of a 5×3 SMA springs array prototype and attached platform. Each SMA spring has 20 mm for length, 0.62 mm for wire diameter and 4.2 mm for nominal diameter. Nylon cord having a length of 40 mm is used to connect SMA springs. The attached platform is composed of beam, bottom case, support plate and various accessories including fan, connection ports and output terminal.

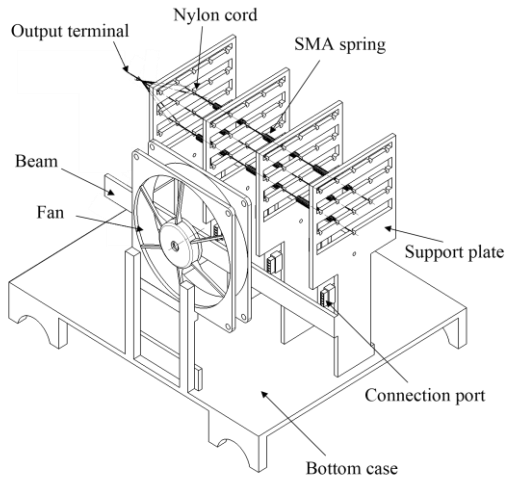

Figure 10. SMA springs array prototype and attached platform

Parameter can be set in GUI to activates SMA springs cells in different locations. SMA springs array starts to contract after clicking "Confirm" in GUI, robot then start to move at a uniform speed in a straight line, and it now moves the force senor along the contraction direction of SMA springs array. Signals from the force sensor are transmitted into LMS SCADAS III frontend, and further sampled and calculated in PC. Activation of SMA springs lasts 5 s and stops after clicking "Off". To account for heat dissipation of SMA springs, the record time of force signals is set to 20 s. The robot moves the force sensors about 3 mm/s, lasts 5 s. Figure 11 shows the action time table for experiment runs.

There are 55 times of experiment. Table II presents the numbers of activated SMA spring cells in each experiment run. Where, M1-M5 respectively represent amount of activated SMA springs in each row.

Event	Time/s	5	10	15	21
Force meaurement	20 s				
SMA activation	7 s				
Robot motion	5 s				

Figure 11. Action time table for experiment runs

TABLE II. DIFFERENT EXPERIMENT RUNS WITH DETAIL OF ACTIVATED SMA SPRING CELLS

Order	Sum of M1-M5	M1	M2	M3	M4	M5
run 1	1	1	0	0	0	0
run 2	2	1	1	0	0	0
run 3	2	2	0	0	0	0
run 4	3	1	1	1	0	0
run 5	3	1	2	0	0	0
run…	…	…	…	…	…	…
run 55	14	2	3	3	3	3
run 56	15	3	3	3	3	3

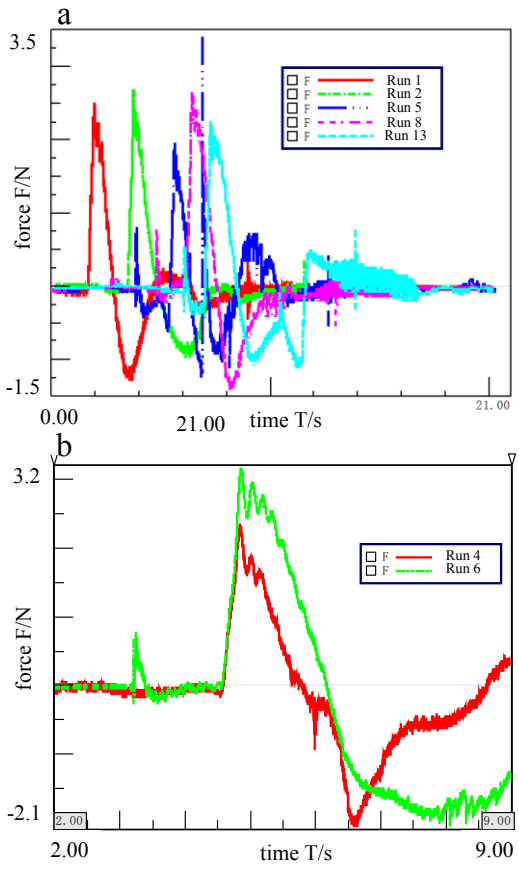

Figure 12. Test resuts. (a) Tension of SMA springs array, where, numbers of activated cells in run1, run2, run5, run8 and run13 respectively equal to 1, 2, 3, 4, 5; (b) an enlarged view of tension signals profile in a time range from 2 s to 9 s, and numbers of activated cells are both equal to 3 in run 4 and run 6.

Figure 12(a) shows the represents the tension curves of the SMA springs array with different activated cells on tensile. As shown here, the measured tension of SMA springs array changes from maximum 3.5 N to minimum -1.5 N, and the maximum difference is equal to 5.0 N. The tensile of the SMA

springs array attenuates in the course of the array contract, which can be divided into four stages. In the case of run 1, the peak tensile of SMA springs array is roughly 0 N in the first stage, roughly 2.5 N in the second stage, roughly 1.3 N in the third stage, and returns to roughly 0 N in the fourth stage. There is no insignificant difference in curves of the between the five runs, and this indicates a serious coupling phenomenon within the SMA springs array.

Figure 12(b) shows an enlarged view of tension signals profile in run 4 and run6. The values of (MI, M2, M3, M4, M5) of run 4 and run 6 is respectively (1, 1, 1, 0, 0) and (3, 0, 0, 0, 0). As shown here, tension in both run 4 and run 6 peaks at about the same time. Run 6 has a relatively larger amplitude than run 4 in the first two stages. In contrast, run 4 has a larger amplitude than run 6 in the third stage. That means SMA springs array has different output properties due to different locations of activated SMA spring cells, even if they have the same numbers of activated SMA spring cells.

VI. CONCLUSION

In this paper the development of control system for a SMA springs array is presented. The design aimed at demonstrating the possibility of biological inspired signal and energy flow control, to gain both applying PLC based control device and Kingview based GUI. The results obtained in the work already done allow us to state that the biomimetic control method adapt to this kind of application. The design provides easy adjustment and rapid response for control of SMA springs array.

REFERENCES

[1] K. J. Cho, J. Rosmarin, and H. Asada, “SBC Hand: A Lightweight Robotic Hand with an SMA actuator Array implementing C-segmentation,” in IEEE International Conference on Robotics and Automation, Roma, Italy, 2007.

[2] S. Mao, E. Dong, H. Jin, M. Xu, S. Zhang, J. Yang, and K. H. Low, “Gait Study and Pattern Generation of a Starfish-Like Soft Robot with Flexible Rays Actuated by SMAs,” Journal of Bionic Engineering, vol. 11, no. 3, pp. 400–411, 2014.

[3] P. Arena, L. Fortuna, M. Frasca, and G. Vagliasindi, “A wave-based CNN generator for the control and actuation of a lamprey-like robot,” International journal of bifurcation and chaos in applied sciences and engineering, vol. 16, no. 1, pp. 39-46, 2006.

[4] J.-S. Koh, and K.-J. Cho, “Omega-Shaped Inchworm-Inspired Crawling Robot With Large-Index-and-Pitch (LIP) SMA Spring Actuators,” IEEE-ASME Transactions on Mechatronics, vol. 18, no. 2, pp. 419-429, 2013.

[5] S. Kim, E. Hawkes, K. Cho, M. Joldaz, J. Foleyz, and R. Wood, "Micro artificial muscle fiber using NiTi spring for soft robotics." pp. 2228 -2234

[6] S. Ying, S. Ji, Z. Wang, and Z. Fan, “Output Properties of Cellular Artificial Actuator,” in IEEE International Conference on Robotics and Biomimetics (ROBIO), 2013, pp. 2369 - 2373.

[7] K. J. D. Laurentis, A. Fisch, J. Nikitczuk, and C. Mavroidis, "Optimal Design of Shape Memory Alloy Wire Bundle Actuators." pp. 2363-2368.

[8] M. J. Mosley, and C. Mavroidis, “Experimental non-linear dynamics of a shape memory alloy wire bundle actuator,” Journal of Dynamic Systems, Measurement, and Control(Transactions of the ASME), vol. 123, no. 1, pp. 103-112, 2001.

[9] N. M. Rey, R. M. Miller, T. G. Tillman, R. M. Rukus, and J. L. Kettle, Shape memory alloy bundles and actuators, US 20050150223, U. S. P. Application, 2005.

[10] F. Rothling, R. Haschke, J. J. Steil, and H. Ritter, "Platform portable anthropomorphic grasping with the bielefeld 20-DOF shadow and 9-DOF TUM hand." pp. 2951-2956.

[11] D. MacNair, and J. Ueda, “Modeling & characterizing stochastic actuator arrays,,” in International Conference on Intelligent Robotsand Systems, 2009, pp. 3232–3237.

[12] D. MacNair, and J. Ueda, “A fingerprint method for variability and robustness analysis of stochastically controlled cellular actuator arrays,” The International Journal of Robotics, vol. 30, no. 5, pp. 536–555, 2011.

[13] www.picstopin.com. "motor neuron model."